Investigating the sensitivity of surface-level nitrate seasonality in Antarctica to primary sources using a global model

Hyung-Min Lee [a], Daven K. Henze [b,*], Becky Alexander [c], Lee T. Murray [d,e]

[a] Department of Civil, Environmental, and Architectural Engineering, University of Colorado, Boulder, CO 80309, USA
[b] Department of Mechanical Engineering, University of Colorado, Boulder, CO 80309, USA
[c] Department of Atmospheric Sciences, University of Washington, Seattle, WA 98195, USA
[d] School of Engineering and Applied Sciences, Harvard University, Cambridge, MA 02138, USA
[e] Lamont-Doherty Earth Observatory, Columbia University, Palisades, NY 10964, USA

HIGHLIGHTS

- Model simulations are used to assess sources of TNIT ($HNO_3 + NO_3^-$) in Antarctica.
- Adjoint analysis is used to evaluate impacts of surface versus stratospheric sources.
- TNIT in May–July is attributed to HNO_3 from NO_x emissions as far north as 25°S.
- In other seasons, TNIT is transported in the form of PAN.
- PSC sedimentation may contribute to observed peaks in concentrations in August.

ARTICLE INFO

ABSTRACT

Determining the sources of total nitrate (TNIT $\equiv NO_3^- + HNO_3$) reaching Antarctica is a long-standing challenge. Here we analyze the monthly sensitivity of surface-level TNIT in Antarctica to primary sources using a global 3-D chemical transport model, GEOS-Chem, and its adjoint. Modeled seasonal variation of TNIT concentrations shows good agreement with several measurement studies, given that the lack of post-depositional processing in the model leads to an expected underestimate of maximum values in November through January. Remote NO_x sources have the greatest impact May–July, during when the model background concentrations are sensitive to NO_x emissions from fossil fuel combustion, soil, and lightning originating from 25°S to 65°S. In this season, NO_x is transported to Antarctica as TNIT, which is formed above continental source regions at an altitude of 5–11 km. In other seasons, more NO_x is transported as a reservoir species (e.g., peroxyacetyl nitrate, PAN) through the free troposphere, transforming into TNIT within a cone of influence that extends to 35°S and above 4 km altitude. Photolysis of PAN over Antarctica is the main driver of modeled NO_x seasonality. Stratospheric production and loss of tracers are relatively unimportant in monthly sensitivities in GEOS-Chem, driving only a few percent of surface level variability of TNIT. A small peak concentration in August is captured by the model, although some measured values in August fall outside the range of simulated concentrations. Modifications to the model to represent sedimentation of polar stratospheric clouds (PSCs) lead to increased surface level August TNIT concentrations. However, this simple representation does not explicitly account for PSC particle deposition or disappearance of the tropopause in the middle of winter, and thus the influence of stratospheric nitrate sources estimated in this study is likely a lower bound.

© 2014 Elsevier Ltd. All rights reserved.

1. Introduction

TNIT ($\equiv NO_3^- + HNO_3$) is an oxidation product of nitrogen oxides ($NO_x \equiv NO + NO_2$) in the atmosphere associated with important environmental issues such as aerosol concentrations and the oxidative capacity of the atmosphere. A significant fraction of NO_x is sequestered as TNIT and then removed from the atmosphere by wet

and dry deposition, providing nitrogen to the surface where it serves as a key ecosystem nutrient. Given its environmental importance, there are interests in understanding past variability of atmospheric NO_x. Numerous studies have reported seasonal and historical variations in TNIT concentrations in Antarctica, yet the mechanisms and sources driving these variations are still not well quantified.

As a proxy for historical variability of atmospheric NO_x, ice cores from polar regions provide chronologically preserved records of TNIT (Wilson and House, 1965; Legrand et al., 1988; Mayewski and Legrand, 1990; Legrand and Kirchner, 1990; Jacobi et al., 2000; Jones et al., 2011; Wolff et al., 2012). Greenland ice core NO_3^- records show that the Northern Hemispheric NO_3^- burden has doubled since the mid twentieth century due to anthropogenic emissions (Mayewski et al., 1986). In contrast, impacts of human activity on NO_3^- are not as prominent in Antarctic ice cores (Mayewski and Legrand, 1990). Aerosol measurements at the surface are also used to constrain recent trends and seasonal variability of nitrate (Savoie et al., 1993; Wagenbach et al., 1998; Weller et al., 2002; Savarino et al., 2007; Jones et al., 2008). Antarctic measurements consistently show minimum levels of TNIT in April–June, a small peak in August, and a steady increase afterward until maximum levels are reached in November–January (Savoie et al., 1993; Savarino et al., 2007; Jones et al., 2011; Weller et al., 2011).

To interpret the significance of Antarctic ice-core and aerosol measurements, three important types of processes that influence Antarctic surface-level TNIT must be considered. First, variations in TNIT burden are impacted by long-range tropospheric transport of species emitted outside Antarctica. Emissions of NO_x include surface sources (fossil fuel, biofuel, soil exhalation, biomass burning), lightning, and aircraft emissions. TNIT may be transported directly, as NO_x or aerosol nitrate, or as reservoir species such as peroxyacetyl nitrate (PAN). PAN is produced by chemical reactions between hydrocarbons and NO_x and has a highly temperature dependent lifetime (1 h at 298 K, 5 months at 250 K). Once it ascends to the free troposphere, it can be transported to the polar regions and then decomposed upon descent into NO_x by thermal decomposition or photolysis (Mills et al., 2007; Jacobi et al., 2000; Jones et al., 2011).

Second, stratospheric influences in Antarctic TNIT include sedimentation of polar stratospheric clouds (PSCs) and HNO_3-rich airmass mixing across the tropopause. One of the major components of PSCs is HNO_3 (Carslaw et al., 1995; Pitts et al., 2007). The polar vortex provides a favorable environment for PSCs to form and grow; subsequent sedimentation of PSCs is responsible for removal of gas-phase HNO_3 in winter from the Antarctic stratosphere, i.e., denitrification (Fahey et al., 1990; Carslaw et al., 1994). Also, an enhanced polar vortex can result in disappearance of the tropopause above Antarctica (Rubin, 1953) leading to more active airmass mixing between the stratosphere and troposphere (Savoie et al., 1993; Wagenbach et al., 1998; Weller et al., 2002).

Lastly, TNIT deposited on snow can recycle several times by re-emission to the atmosphere by HNO_3 evaporation or photochemical reduction into NO_x (Weller et al., 2004; Savarino et al., 2007; Jones et al., 2008). This process, so called post-depositional processing, has been suggested to cause observed TNIT maximum concentrations in late spring and early summer (Savarino et al., 2007; Jones et al., 2008; Weller et al., 2011).

The variety and complexity of these sources and mechanisms make it challenging to relate observed Antarctic TNIT to atmospheric NO_x (Zeller and Parker, 1981; Röthlisberger et al., 2000; Savarino et al., 2007; Wolff et al., 2008). While local meteorology and post-depositional processing influence the high TNIT concentrations in summer by active photochemistry within Antarctica, the original source of TNIT for this recycling remains to be quantified

(Wolff et al., 2008). Specifically, it is of interest to determine the contribution of continental emissions versus stratospheric input, the role of different types of natural versus anthropogenic emissions, and the chemical mechanisms by which TNIT is processed and transported to Antarctica in the troposphere.

Atmospheric chemical transport models provide a means of investigating the importance of possible sources of Antarctic TNIT. Although there have been modeling studies investigating atmospheric transport towards Antarctica (Krinner and Genthon, 2003; Stohl and Sodemann, 2010), most have been limited to non-reactive tracers (e.g., black carbon, radon) and thus focused on transport of airmass and decay of tracers. A more comprehensive modeling study, considering critical processes for reactive tracers such as chemical reactions, emissions, and dry deposition, has been conducted for Antarctic CO (van der Werf et al., 2013). However, due to the complicated characteristics of NO_x chemistry and transport, there has not to our knowledge been a comprehensive modeling attempt at analyzing sources of Antarctic TNIT until now.

In this study, we use the global 3-D chemical transport model GEOS-Chem and its adjoint to quantify sensitivities of surface level Antarctic TNIT to its precursor processes. These include emissions, and production and loss of tracers resulting from tropospheric and stratospheric chemistry. In doing so, we evaluate the model by comparing the modeled seasonality with measurements from previous studies, although we expect the model to underestimate austral summer observations due to a lack of post-depositional processing in the model.

2. Model description

We use GEOS-Chem (Bey et al., 2001) version 8-02-04 with updates described below to estimate the TNIT concentrations over Antarctica. GEOS-Chem is a global 3-D atmospheric chemical transport model driven by meteorological input from the Goddard Earth Observing System (GEOS) of the NASA Global Modeling and Assimilation Office (www.geos-chem.org). The version of the model employed in this study uses GEOS-5 meteorological fields at $2°$ latitude $\times$ $2.5°$ longitude horizontal resolution, with 47 vertical layers up to 0.01 hPa. The model's tropospheric chemical mechanism consists of more than 290 reactions and 90 gas and aerosol species. Aerosols are assumed to be externally mixed. $SO_4^{2-}-NO_3^--NH_4^+$ thermodynamic equilibrium is calculated using RPMARES (Park et al., 2004), which is based on the MARS-A routine of Binkowski and Roselle (2003). More comprehensive aerosol treatment including sea-salt (Na^+ and Cl^-) and crustal ions (K^+, Ca^{2+}, and Mg^{2+}) is available using another thermodynamic scheme in the model, i.e., ISORROPIA, however, we use RPMARES due to the lack of an adjoint of ISORROPIA until very recently (Capps et al., 2012). Carbonaceous and size-resolved dust aerosols are based on Chin et al. (2002), Park et al. (2003), and Fairlie et al. (2007). Wet deposition includes sub-grid scavenging in convective updrafts, large scale in-cloud rainout and below-cloud washout (Liu et al., 2001). Dry deposition is calculated using a resistance-in-series model (Wesely, 1989; Wang et al., 1998).

A new stratospheric chemistry scheme is implemented for this study. The standard version 8-02-04 of GEOS-Chem applies zonal mean production and loss rates to 23 gaseous species, as archived from earlier 2-D models (Bey et al., 2001). The new linearized stratospheric chemistry (Murray et al., 2012), updated in the adjoint model as well for this study, uses monthly climatological 3-D production and loss rates from the GMI (Global Modeling Initiative) Combo model (http://gmi.gsfc.nasa.gov) for 24 gaseous tracers above the tropopause, including CO, O_3, NO_x, and HNO_3. These production and loss rates only reflect gas-phase chemistry.

Stratospheric O_3 chemistry is treated using the Linoz scheme (McLinden et al., 2000; Liu et al., 2009).

Fig. 1 shows the monthly variation of NO_x emissions summed over 15°S–90°S from the following emission inventories. EDGAR 3.2-FT2000 is used for fossil fuel combustion (Olivier et al., 2005) and GFED2 for biomass burning emissions (van der Werf et al., 2009). Biofuel sources are based on Yevich and Logan (2003), lightning is based on Murray et al. (2012), and soil and aircraft emissions are described in Sauvage et al. (2007). Fossil fuel combustion is fixed throughout the year, and the magnitude of biofuel and aircraft emissions in this latitude range are negligibly small. Biomass burning has a maximum in late winter and early spring (August and September). Lightning and soil emissions are higher from spring to summer and lower from fall to winter.

We use the GEOS-Chem adjoint model (Henze et al., 2007) to evaluate the sensitivity of TNIT reaching the surface level of Antarctica to precursor emissions and stratospheric production and loss rates. The GEOS-Chem adjoint model has been used previously for source attribution (e.g., Kopacz et al., 2011; Walker et al., 2012; Paulot et al., 2012; Parrington et al., 2012) and data assimilation using remote sensing or in-situ observations (e.g., Henze et al., 2009; Kopacz et al., 2010; Jiang et al., 2011; Wecht et al., 2012). The adjoint, a receptor-based sensitivity model, is a very efficient tool for quantifying the sensitivity of a scalar forward model estimate to numerous model parameters. The normalized sensitivity is defined as

$$\lambda_p \equiv \frac{\partial J(c_i)}{\partial p} \cdot \frac{p}{J(c_i)} \qquad (1)$$

where $\partial J(c_i)/\partial p$ is found from solution of the adjoint model. Here c_i is the concentration of species i and $J(c_i)$ is a scalar function of forward model estimates. In this study, $J(c_i)$ is defined as the weekly average TNIT concentration evaluated in flux units over Antarctica at the surface level, i.e., J_{TNIT}. The flux unit here is the total mass of TNIT in the first level of the model per surface area per hour. Considering that the surface area of Antarctica varies during the course of a year as sea ice expands and melts (Stohl and Sodemann, 2010), we determine Antarctica as the land or ice south of 60°S according to the GEOS-5 land-water indices. λ_p is the sensitivity of $J(c_i)$ with respect to the model parameters (p). p in this study consists of emissions of all tracers from various sectors (e.g., fossil fuel, lightning NO_x, natural NH_3, etc.), and stratospheric production and loss rates. In addition, sensitivities with respect to reaction rates (i.e., kinetic reaction rates, deposition rates, photolysis rates, and hydrolysis rates) are also calculated. We performed adjoint simulations for each month from March 2006 to February 2007.
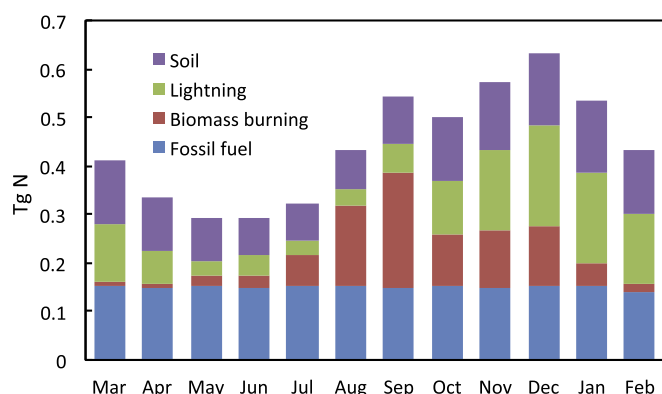
J_{TNIT} is evaluated over the final week of each month and percent contributions are summed globally throughout the month.

3. Results

3.1. Seasonal variations of total nitrate

We first compare seasonal variations of surface level TNIT concentrations estimated from GEOS-Chem with measurement studies in Fig. 2, with additional details on the measurements provided in Table 1. From each of the yearly measurement studies, we extract and plot data relevant to three key observed features: the fall minimum, the August peak, and the maximum (Savoie et al., 1993; Savarino et al., 2007; Jones et al., 2011; Weller et al., 2011). Symbols are placed in the middle of the period that they represent. Given the differences in the locations of these measurements, the species measured (NO_3^-, HNO_3, or TNIT), and the area these measurements represent compared to the size of the model grid cell, we primarily make qualitative comparisons between them and the model estimates.

Measured concentrations show large variations from study to study. It is possible that differences are owing to variations in local conditions (e.g., meteorology, topography, post-depositional processes) and measurement methods. We focus our analysis on TNIT rather than NO_3^- and HNO_3 separately, as thermodynamic partitioning between NO_3^- and HNO_3 in the model may be biased, underestimating NO_3^- due to lack of sea-salt and crustal ions. Considering a dataset that includes both separately (Jourdain and Legrand, 2002), NO_3^- constitutes 67% of the minimum TNIT, 50% of the August TNIT peak, and 34% of the maximum TNIT. Based on this observed partitioning we convert NO_3^- measurements to TNIT concentrations for the other studies shown in Fig. 2. Measured minima and August peaks lie within the modeled first and third quartiles of simulated values over Antarctica. As expected, the model considerably underestimates the maximum in November to January that is thought to be due to post-depositional processing (Savarino et al., 2007; Jones et al., 2008; Weller et al., 2011). The model reasonably represents the magnitude of the August peak even though GEOS-Chem has no scheme describing PSC formation and sedimentation. PSC sedimentation has been suggested as a source of the
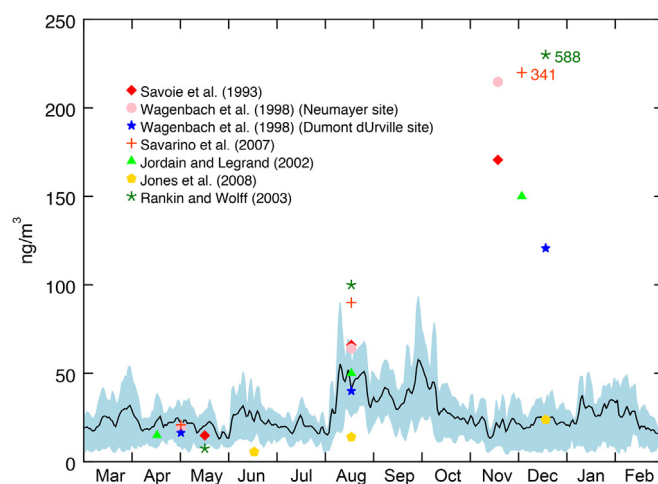

Fig. 2. Modeled TNIT concentration from March 2006 to February 2007 with measurements in symbols. The solid black line is the hourly TNIT concentration averaged over Antarctica (60°S–90°S, see text for details) and shadings indicate first and third quartiles. Two measurements are indicated with values as they are too high to show on the same y-axis. NO_3^- measurements are converted to TNIT concentrations based on the partitioning in Jourdain and Legrand (2002).

Fig. 1. Monthly NO_x emissions for 15°S–90°S from March 2006 to February 2007.

Table 1
Surface air nitrate measurements from previous studies.

Site (tracer)	Minimum	August peak	Maximum	Time
Mawson[a] (NO_3^-)	May (10 ng/m^3)	33 ng/m^3	Nov (58 ng/m^3)	1987–1991
Neumayer[b] (NO_3^-)	Apr–May (13 ng/m^3)	32 ng/m^3	Nov (73 ng/m^3)	1983–1996
Dumont d'Urville[b] (NO_3^-)	Apr–May (11 ng/m^3)	20 ng/m^3	Nov–Jan (41 ng/m^3)	1991–1995
Dumont d'Urville[c] (NO_3^-)	Mar–Jun (14 ng/m^3)	45 ng/m^3	Nov–Dec (116 ng/m^3)	2001
Dumont d'Urville[d] (NO_3^-)	Apr (12 ng/m^3)	25 ng/m^3	Nov–Dec (55 ng/m^3)	2000–2001
Dumont d'Urville[d] (HNO_3)	Apr (5 ng/m^3)	25 ng/m^3	Dec (95 ng/m^3)	2000–2001
Halley[e] (TNIT)	Jun (2 pptv)	5 pptv	Dec (8.5 pptv)	2004
Halley[f] (NO_3^-)	May (∼5 ng/m^3)	50 ng/m^3	Dec (200 ng/m^3)	2001

[a] Savoie et al. (1993).
[b] Wagenbach et al. (1998).
[c] Savarino et al. (2007).
[d] Jourdain and Legrand (2002).
[e] Jones et al. (2008).
[f] Rankin and Wolff (2003).

August peak or the spring maximum (Mayewski and Legrand, 1990; Wagenbach et al., 1998; Savarino et al., 2007). It is still ambiguous from these results whether PSC sedimentation has a small effect on the August peak or its impact on surface level TNIT appears in spring not in August. This issue is considered further in Section 3.2.2.

The spatial distributions of modeled TNIT at the surface level are shown in Fig. 3. For all seasons, East Antarctica has a higher mixing ratio than West Antarctica, and the mixing ratio in the Northeast is higher than in the Southwest. As shown in Fig. 3, the spatial distribution of TNIT is similar to the boundary layer top pressure distribution which corresponds to topography (lower pressure to higher topography). The effects of topography will cause spatial variations in accumulation rate, which is expected to impact TNIT concentrations via post-depositional processing (Ritz et al., 2001; Arthern et al., 2006).

3.2. Source attribution of total nitrate (TNIT)

To better understand the factors governing the abundance of TNIT, we comprehensively diagnose the sensitivity of J_{TNIT} to sources using the GEOS-Chem adjoint. Table 2 shows the three sources with the largest percent contribution ($\lambda_p \times 100\%$) to J_{TNIT} in each month, and Fig. 4 shows the spatial distribution of sources to which J_{TNIT} is sensitive. For example, in the final week of March, the average TNIT flux to the Antarctic surface, i.e., J_{TNIT}, is 3.7 μg/m^2 hr. Over the course of the entire month, NO_x emissions from fossil fuel combustion contribute the most to J_{TNIT}, responsible for a 5.3% increase, and stratospheric loss of HNO_3 is responsible for a 4.4% decrease of J_{TNIT}.

While the source contributions in Table 2 and Fig. 4 show the ultimate sectors and locations of origin, they alone do not answer questions such as: which NO_x reservoir species are most responsible for transport to Antarctica, and what is the role of chemical reactions during transport? To answer these questions we quantify the roles of different chemical mechanisms transforming NO_x by calculating sensitivities of J_{TNIT} with respect to chemical reaction rate constants. Among 24 reactions directly producing HNO_3, three reactions, (R1)–(R3), are found to contribute the most, in agreement with Alexander et al. (2009),

$$NO_2 + OH \rightarrow HNO_3 \qquad (R1)$$

$$N_2O_5 + H_2O \rightarrow 2HNO_3 \qquad (R2)$$

$$NO_3 + DMS \rightarrow HNO_3 \qquad (R3)$$
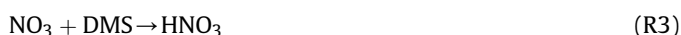
where DMS is dimethylsulfide. Table 3 shows the globally integrated sensitivities with respect to (R1)–(R3). The relative importance of each reaction varies by season and is affected by a combination of emissions, chemistry, and meteorology. Although these are HNO_3-producing pathways, their contributions often exhibit negative values when more HNO_3 is lost than added to J_{TNIT}. This occurs when the net HNO_3 produced by a given pathway occurs too far from Antarctica for the HNO_3 to reach the continent prior to being removed from the atmosphere by deposition. Figs. 5 and 6 map the horizontal and vertical distribution of each reaction's contribution to J_{TNIT}. It is evident that when the reactions occur too far away from Antarctica, a source of J_{TNIT} is removed from the atmosphere. The lifetime of HNO_3 is short, about 2–5 days in the lower atmosphere, because it is readily removed near the surface by wet and dry deposition. Meanwhile, when these reactions occur closer to Antarctica they positively contribute to J_{TNIT}, showing that if the precursors involved in (R1)–(R3) reach certain latitudes the resulting HNO_3 will be transported to Antarctica. There is a vertical transition above the mid-latitudes where continental sources are emitted; if precursors ascend across this transition then the HNO_3 they form will be transported to Antarctica. The critical altitude appears to be ∼4 km, extending as far north as 40°S.

Surface level TNIT shows small positive sensitivities (less than 1%) to stratospheric production of tracers in most months. However, additional calculations at the 4° latitude × 5° longitude resolution show that long-term (6 month) integration of the adjoint sensitivities lead to positive sensitivities that are twice as large as those from 1-month integration, with no significant increase of sensitivities after 6 months. Thus, sensitivities to the stratospheric production from the month long, 2° × 2.5° resolution analysis shown in Table 2 may be an underestimate. In contrast, sensitivities with respect to emissions and stratospheric loss appear to converge within one month.

3.2.1. Background concentrations

The lowest J_{TNIT} values of 1.8 μg/m^2 hr appear in May and July; During these months, the sensitivities are consistently dominated by fossil fuel, and then soil and lighting NO_x emissions with negligible sensitivities to stratospheric loss (Table 2). We therefore consider the modeled minimum concentrations as extending from May through July. And these minimum levels are regarded as background concentrations. The range of background concentrations across Antarctica are in good agreement with observations (Fig. 2). Spatially, the origin of those sources are shown in Fig. 4. Influential NO_x emissions are distributed from 30°S to 65°S. Regarding emissions, biomass burning is greater than lightning NO_x in July, however lightning NO_x is still the third most influential source. NO_x from biomass burning originates in lower latitudes between 10°S and 30°S and at the surface, whereas lightning NO_x is produced in higher latitudes and altitudes where it can be effectively transported to Antarctica.
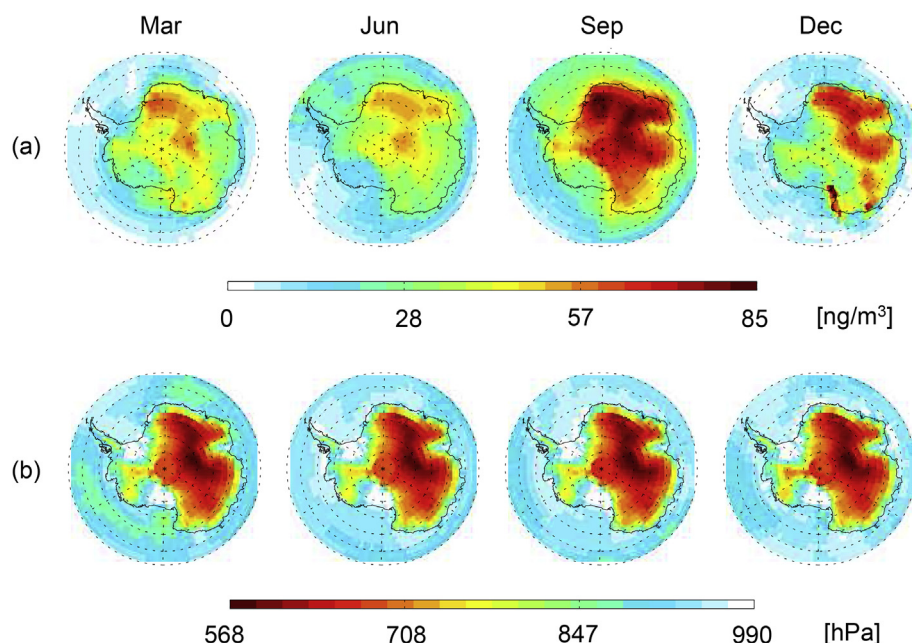
Fig. 3. Monthly average (a) surface level concentration of TNIT estimated by GEOS-Chem and (b) boundary layer top pressure (62°S–90°S).

Total influences of reactions producing HNO_3 (R1–R3) are all negative from April to August (Table 3). Due to a lack of sunlight from the end of March through the next six months, there is no local supply of OH radical in Antarctica. Thus, HNO_3 produced by (R1) during the austral winter is not produced locally in Antarctica but is imported from lower latitudes or the stratosphere. Fig. 6 shows that J_{TNIT} is produced from precursors injected into the free troposphere at latitudes as far north as 35°S. O_3 dry deposition (2.7–3.5%), $NO + O_3 \rightarrow NO_2 + O_2$ (1.3–3.1%), and thermal decomposition of PAN (1.4–2.4%) are the most influential reactions during May–July. J_{TNIT} is positively sensitive to these reactions since they favor NO_2, which may be further oxidized to TNIT. Spatial distributions of these reactions are shown in Figs. 7–9. As more O_3 is removed near the surface by dry deposition, less NO_2 is scavenged via $NO_2 + O_3 \rightarrow NO_3 + O_2$, and the chance for NO_2 or PAN to be lofted above the critical altitude is enhanced. NO_2 produced from $NO + O_3 \rightarrow NO_2 + O_2$ over the continents near the surface also favors PAN formation. The same reaction near the tropopause contributes to TNIT in Antarctica, which is affected by high O_3 concentrations from the stratosphere. If the reaction occurs at altitudes between the two positively sensitive regions, the resulting NO_2 does not add TNIT to Antarctica but deposits in the Southern Ocean. Thermal decomposition of PAN is influential during austral fall and winter, increasing with increasing temperature towards the troposphere from the stratosphere. It occurs at altitudes lower than 6 km and photolysis of PAN occurs at higher altitudes, up to 12 km. Considering that J_{TNIT} is positively sensitive to PAN formation in the mid-latitudes (30°S–50°S) and that thermal decomposition occurs throughout the free troposphere (Figs. 8 and 9), we conclude that PAN produced in the mid-latitudes and transported through the free troposphere can be an effective source of TNIT over Antarctica.

3.2.2. Peak concentrations in August

Model estimates and measurements both show a peak in TNIT concentration in August. It is interesting that the model shows high concentrations in August without a scheme describing PSC formation and sedimentation, which has been suggested from measurement studies as being a major source of the peak in August (Mayewski and Legrand, 1990; Wagenbach et al., 1998; Savarino et al., 2007). Decomposition of PAN has also been suggested as a source of NO_x during austral winter to early spring (Savarino et al., 2007; Jones et al., 2011). In this study, thermal decomposition of PAN is the most influential reaction in August, accounting for 2.9% of the positive sensitivity. J_{TNIT} in August is still most sensitive to fossil fuel combustion (7.8%), lightning (3.4%) and soil (3.2%) NO_x emissions from 30°S to 65°S. There is relatively less contribution from continental sources compared to May–July. August marks a transition between the season when remote influences dominate during winter and local reactions dominate during summer.

The sensitivity with respect to stratospheric production of NO_x is 1.6%. Compared to the 0.4–0.6% contribution in May–July, this increased stratospheric NO_x contribution shows that stratospheric influence on the August peak is represented by the model. It is worth pointing out that sensitivities with respect to stratospheric production and loss rates do not equate to the actual fluxes from and to the stratosphere, just the amount by which current stratospheric chemistry influences these fluxes. Thus, a small increase in the stratospheric production rate results in a large increase in the surface level TNIT, since the HNO_3 mixing ratio is significantly higher in the stratosphere compared to the troposphere (Fig. 11). Stratospheric effects seen in GEOS-Chem reflect the climatological production and loss of tracers by gas-phase chemistry in the stratosphere. However, PSC formation and sedimentation is not included in the model. Thus, this stratospheric influence is likely the effect of the polar vortex in conjunction with the lack of photolysis during the austral winter. Noting that the model does not include PSC sedimentation nor the disappearance of the tropopause, these estimates of stratospheric contributions are likely lower bounds.

Although it is well known that PSCs are responsible for removal of gas-phase HNO_3 in the winter in the Antarctic stratosphere, i.e., denitrification (Fahey et al., 1990; Carslaw et al., 1994), whether the effect of PSC sedimentation is detectable in surface level HNO_3 concentrations is still not clear. Fig. 11 shows vertical profiles of HNO_3 from (a) GEOS-Chem and (b) GMI. The major difference between these models is that GMI considers PSC formation and sedimentation whereas GEOS-Chem does not. We therefore
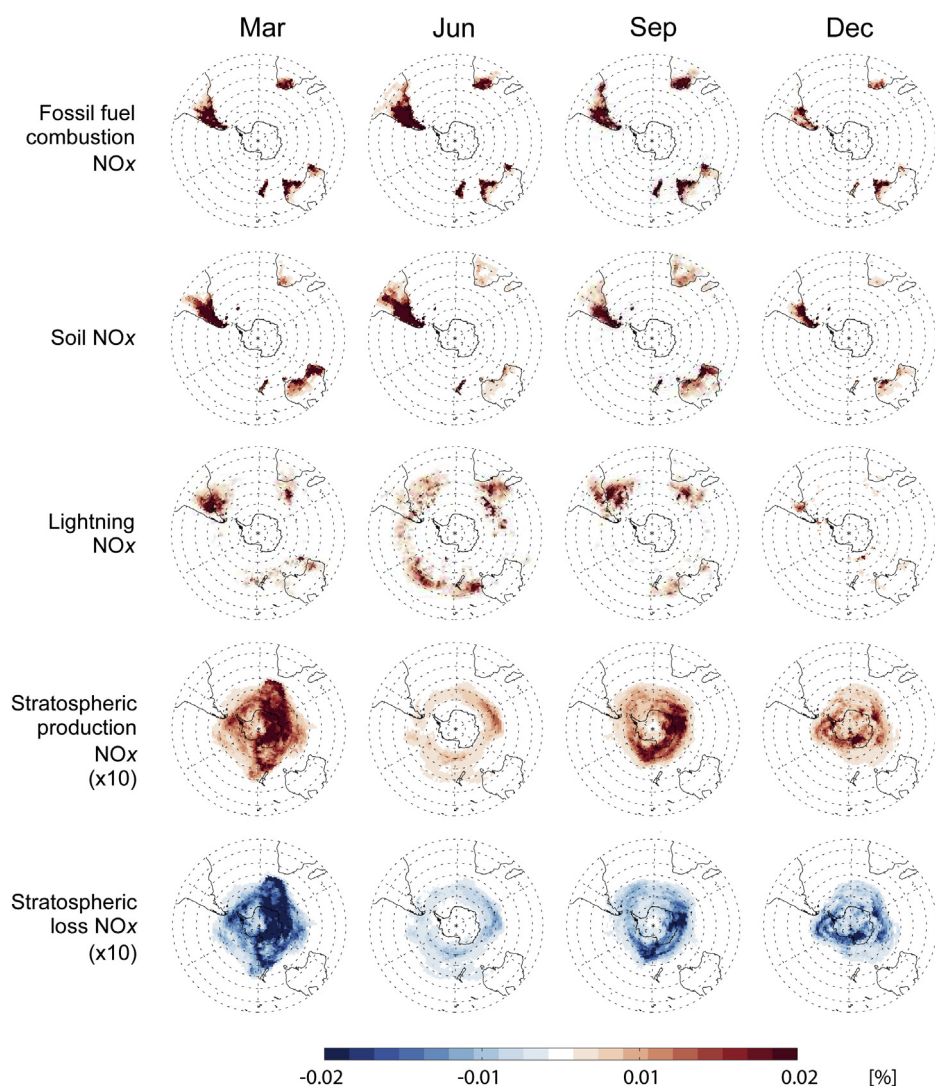
Table 2
Global contributions of emissions and stratospheric tracers to J_{TNIT}.

Month	MAM			JJA			SON			DJF		
	3	4	5	6	7	8	9	10	11	12	1	2
J (μg/m² hr)	3.7	2.9	1.8	2.3	1.8	3.9	4.6	2.3	2.1	2.7	4.0	2.4
Pos (%)	ffNO$_x$ 5.3	ffNO$_x$ 7.6	ffNO$_x$ 12.5	ffNO$_x$ 14.6	ffNO$_x$ 14.6	ffNO$_x$ 7.8	ffNO$_x$ 6.4	ffNO$_x$ 6.9	ffNO$_x$ 4.8	bbNO$_x$ 3.1	spNO$_x$ 3.0	liNO$_x$ 4.6
	soNO$_x$ 5.1	soNO$_x$ 5.8	soNO$_x$ 9.4	soNO$_x$ 8.2	soNO$_x$ 5.1	liNO$_x$ 3.4	soNO$_x$ 3.6	soNO$_x$ 6.7	soNO$_x$ 3.7	soNO$_x$ 2.0	spHNO$_3$ 2.3	soNO$_x$ 2.8
	spHNO$_3$ 4.1	liNO$_x$ 2.7	liNO$_x$ 3.2	liNO$_x$ 5.2	liNO$_x$ 2.9	soNO$_x$ 3.2	liNO$_x$ 3.3	naNH$_3$ 4.2	liNO$_x$ 3.5	ffNO$_x$ 1.9	bbNO$_x$ 2.1	spNO$_x$ 1.8
Neg (%)	slHNO$_3$ −4.4	slNO$_x$ −2.0	slNO$_x$ −1.0	−*	−*	slNO$_x$ −1.4	slNO$_x$ −1.7	slNO$_x$ −1.1	slNO$_x$ −2.6	slNO$_x$ −2.0	slNO$_x$ −3.4	slNO$_x$ −2.1
	slNO$_x$ −4.0	slHNO$_3$ −1.4	−*	−*	−*	−*	−*	−*	slHNO$_3$ −1.2	slHNO$_3$ −1.2	slHNO$_3$ −2.5	slHNO$_3$ −1.7
	slHNO$_4$ −1.8	slHNO$_4$ −1.0	−*	−*	−*	−*	−*	−*	−*	−*	slHNO$_4$ −1.0	−*

– MAM: March April May, JJA: June July August, SON: September October November, DJF: December January February.
– ff: fossil fuel combustion, li: lightning, na: natural, sl: stratospheric loss, so: soil, sp: stratospheric production.
– *: <1.0%.

Fig. 4. Spatial distribution of source contributions to J_{TNIT} (15°S–90°S).

Table 3
Global total contribution of major reactions forming HNO$_3$ to J_{TNIT}.

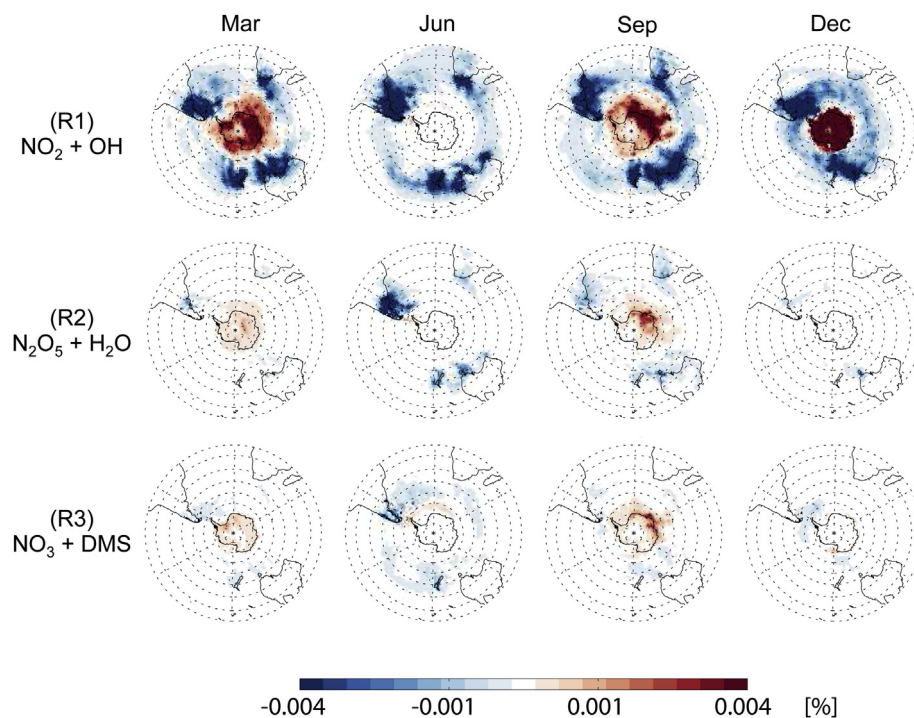| Month	MAM			JJA			SON			DJF		
	3	4	5	6	7	8	9	10	11	12	1	2
(R1) NO$_2$ + OH → HNO$_3$ (%)	1.4	−4.6	−6.3	−4.5	−7.8	−4.1	0.5	9.3	13.5	16.3	11.4	11.5
(R2) N$_2$O$_5$ + H$_2$O → 2 HNO$_3$ (%)	0.8	−0.2	−1.0	−1.0	−2.4	−0.6	0.8	0.4	−0.2	−0.1	−0.1	−0.6
(R3) NO$_3$ + DMS → HNO$_3$ (%)	0.3	−0.4	−0.8	−0.5	−0.6	−0.2	0.7	0.0	−0.4	−0.2	−0.1	−0.3

Fig. 5. Spatial distribution of J_{TNIT} sensitivities to reactions producing HNO_3 (15°S−90°S).
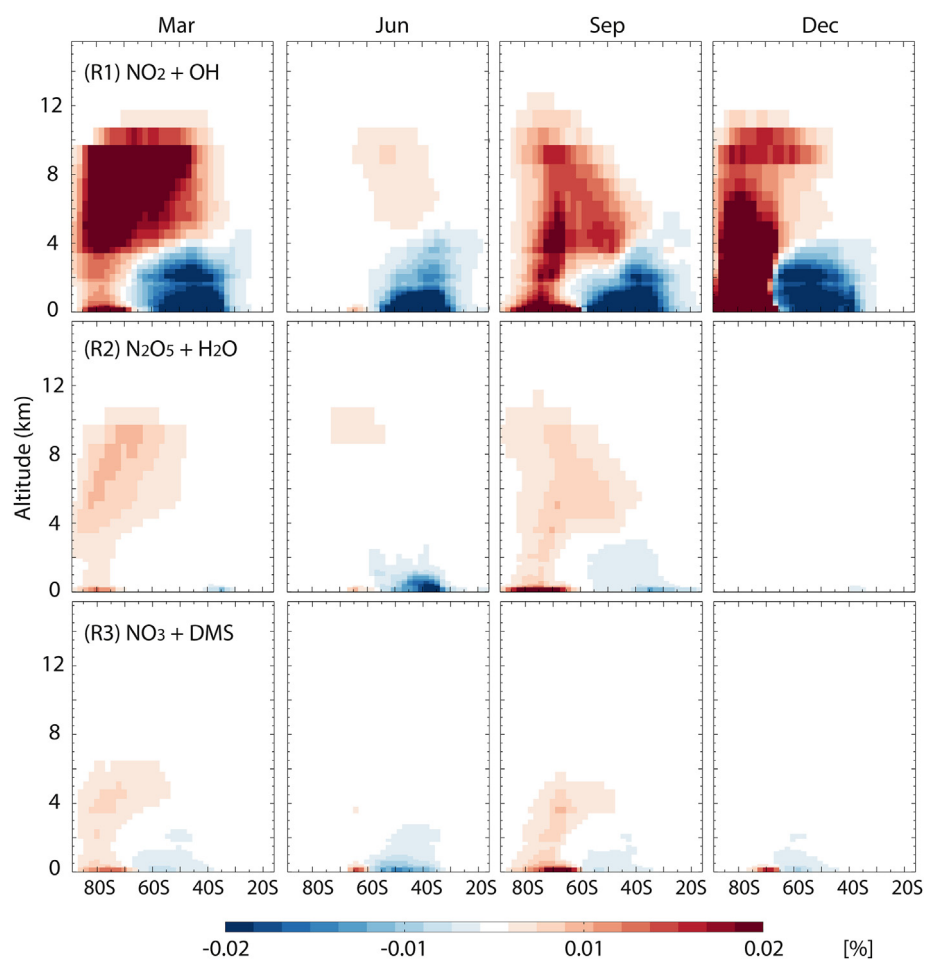
Fig. 6. Vertical distribution of J_{TNIT} sensitivities to reactions producing HNO_3 (15°S−90°S).
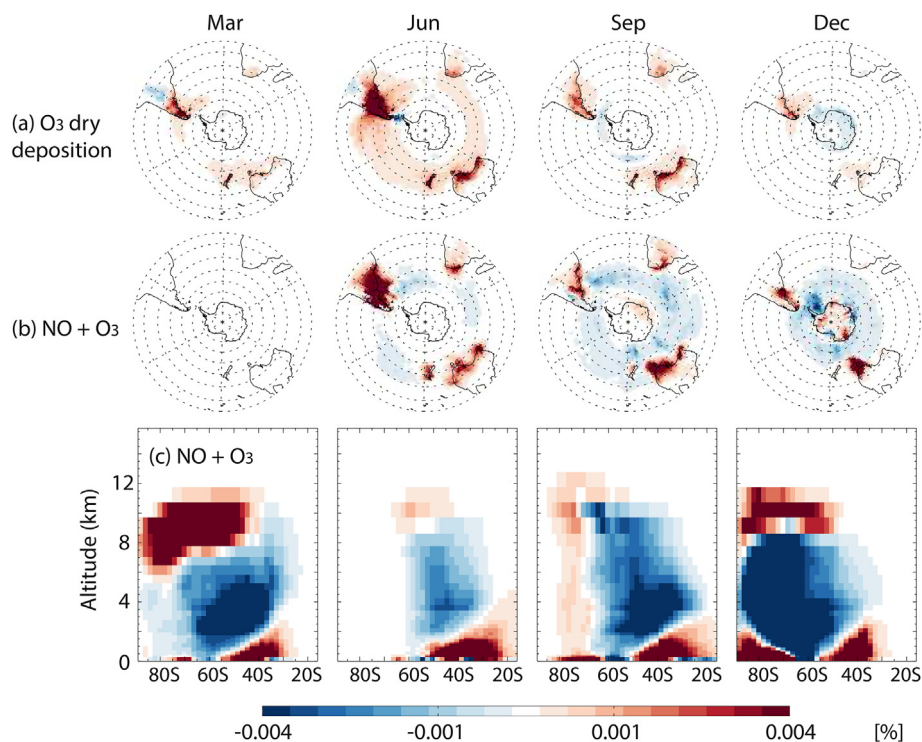
Fig. 7. Horizontal and vertical distribution of J_{TNIT} sensitivities to (a) dry deposition and (b), (c) reaction of NO with O_3.

modified GEOS-Chem to have similar vertical profiles of HNO_3 to that of GMI, see Fig. 11 (c). This profile is achieved by enforced sedimentation of HNO_3 at 14 km altitude, adjacent to the tropopause, from HNO_3 in the 15–25 km range during June to November. This allows us to examine the effect of enhanced HNO_3 mixing ratios in the lower stratosphere (∼140 hPa) on surface level HNO_3 concentrations in GEOS-Chem. With this modification, surface level HNO_3 increases from August through October as shown in Fig. 12, and more measurements of the August peak fall in the range of model estimates with this modification. This result, which does not include particles from PSCs, suggests that effects of PSCs on surface TNIT can be explained largely by gas-phase convection in August. However, the impact in October is smaller than in August and
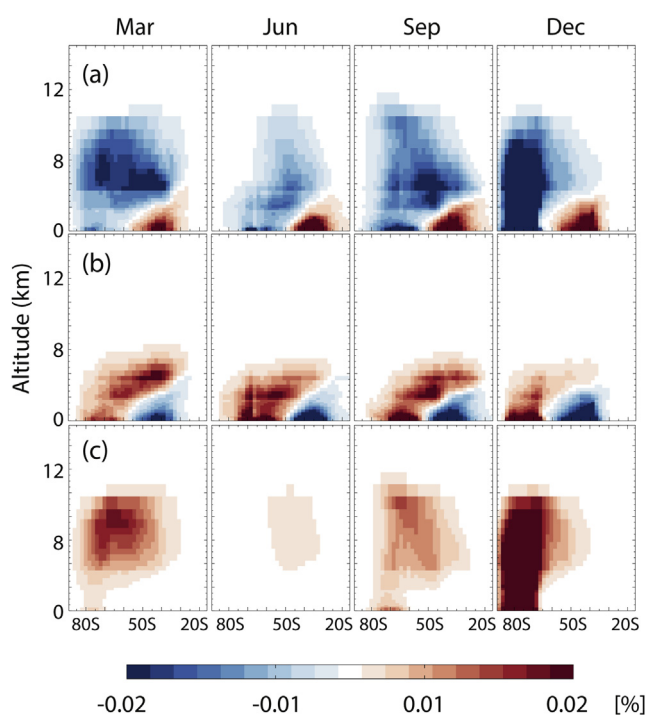
Fig. 8. Vertical distribution of J_{TNIT} sensitivities to the formation and decomposition of PAN (15°S–90°S). (a) PAN formation, (b) thermal decomposition, (c) photolysis.

Fig. 9. Same as Fig. 8 but for horizontal distribution.

Fig. 10. Annual variation of sensitivities of J_{TNIT} to the PAN formation and decompositions.

Fig. 12. Same as Fig. 2 but showing impacts of enforced HNO_3 enhancement in lower stratosphere in GEOS-Chem. From June to November 2006. Blue dash line is the mean and blue solid lines are first and third qua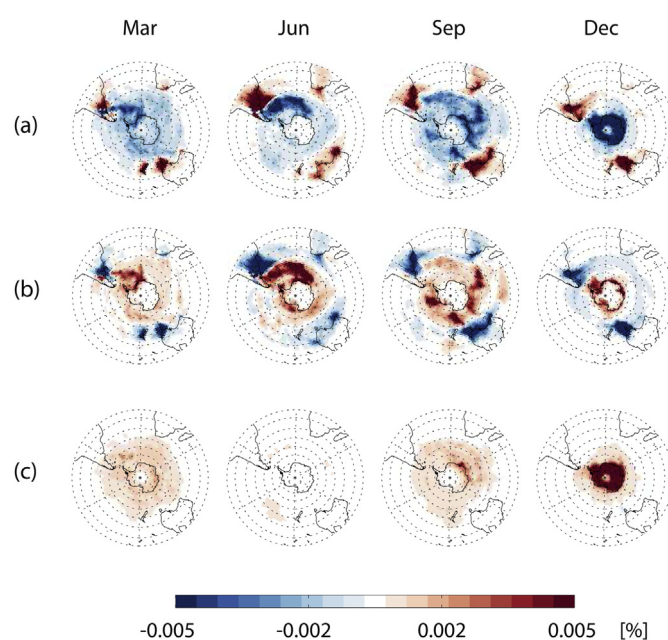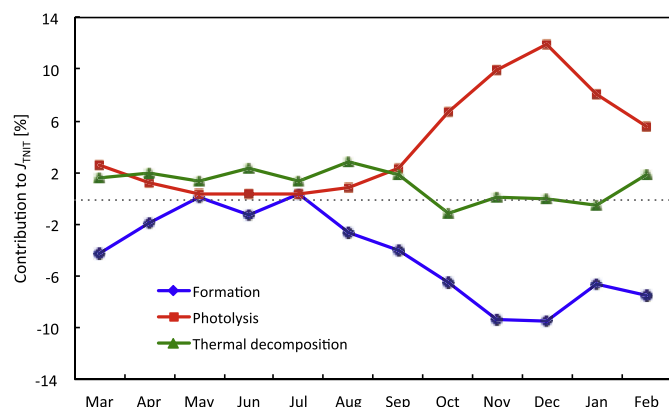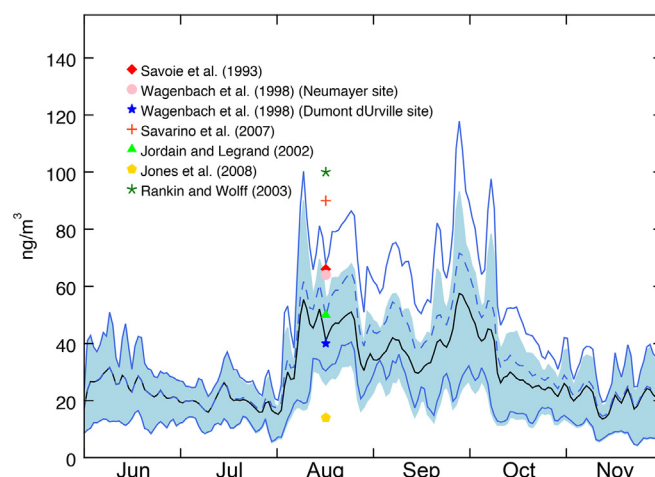rtiles of surface level TNIT concentrations calculated by modified GEOS-Chem. (For interpretation of the references to colour in this figure legend, the reader is referred to the web version of this article.)

September, showing that the gas-phase convection is unlikely a factor controlling the spring maximum.

3.2.3. Maximum concentrations

Modeled maximum TNIT concentrations appear at the end of September, however the concentration is only slightly higher than the August peak (Fig. 2). While measured concentrations at the end of September are comparable to modeled concentrations, the model underestimates the observed maximum concentration in November–January. Measured maximum TNIT concentrations have been attributed to the combination of PSC sedimentation (Wagenbach et al., 1998; Weller et al., 2002; Savarino et al., 2007) and post-depositional processing (Savarino et al., 2007; Jones et al., 2008). Given that the model does not well represent the tropopause in winter, PSC sedimentation, nor post-depositional processing, differences between modeled and measured TNIT concentrations in November to January can be considered as an upper bound on contributions from these mechanisms.

Regarding the sensitivities of modeled maximum TNIT, NO_x emissions from fossil fuel, soil, and lightning are the three most influential sources in September. As Antarctica starts to receive more solar radiation in spring, photochemical reactions become active. J_{TNIT} starts to indicate positive sensitivities to (R1)–(R3) in September (Table 3). PAN photolysis is the most positively influential reaction for the modeled maximum in September. From October to February, modeled J_{TNIT} is consistently affected the most by (R1) (9%–11%) and PAN photolysis (6–12%), indicating strong effects of active photolysis owing to extended daylight hours and enhanced high surface albedo. Thus, implementation of post-depositional

processing, also controlled by photolysis, in the model will likely introduce more TNIT in these months. Comparing the two mechanisms of PAN decomposition in the model, contributions from photolysis dominate compared to thermal decomposition (Fig. 10). Global effects of PAN formation appear to be positive only when it is formed in an area where transport to Antarctica is likely.

Another thing to consider is that GEOS-Chem does not include the heterogeneous chemistry of the stratospheric ozone hole. Thus, O_3 in the polar vortex over Antarctica in austral spring during September to November is greatly overestimated, which will affect the $NO + O_3 \rightarrow NO_2 + O_2$ pathway once O_3 is transported to the troposphere. Therefore, J_{TNIT} in September to November could be overestimated as a consequence of overestimated stratospheric O_3 transported to the troposphere.

4. Summary and conclusions

We have assessed sensitivities of surface level Antarctic TNIT to various emission sectors in the troposphere and production and loss of tracers in the stratosphere throughout a year using GEOS-Chem and its adjoint. Average annual minimum, August peak, and annual maximum TNIT concentrations from measurement studies are compared with modeled TNIT concentrations across Antarctica. Most seasonal minima from measurements lie within
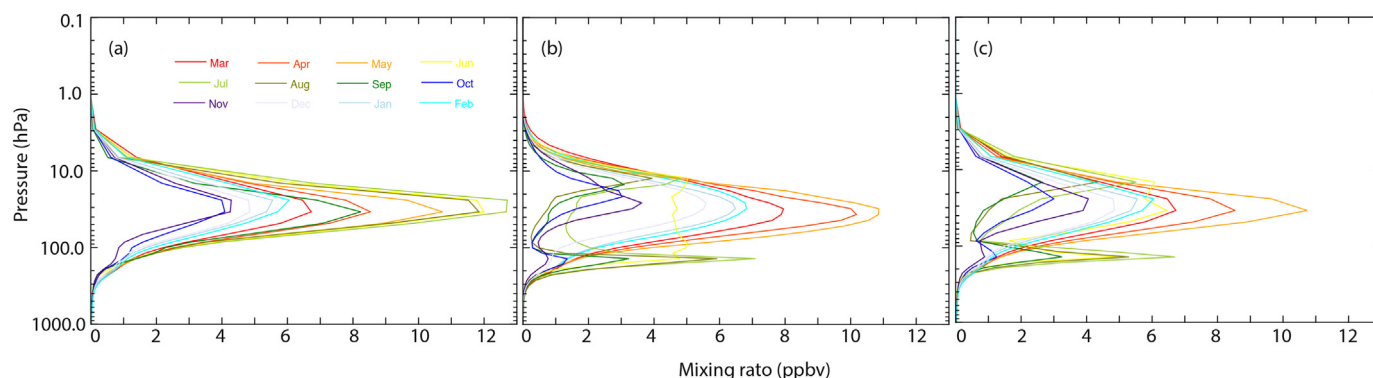
Fig. 11. Monthly HNO_3 vertical profiles averaged over Antarctica (70°S–90°S). (a) GEOS-Chem, (b) GMI, (c) Modified GEOS-Chem.

the first and third quartiles of modeled background concentrations during May to July. The first and relatively small peak of the year appearing in August, i.e., the August peak, is also captured by the model. Representation of the August peak in the model is improved by inclusion of enhanced HNO_3 mixing ratios in the lower stratosphere to mimic the effects of PSC formation and sedimentation. The model is not able to reproduce the maximum concentration of the year observed in November to January likely due to a lack of post-depositional processing. We anticipate this underestimation to be resolved with implementation of new snow chemistry and post-depositional processing (Zatko et al., 2013) in future work. In addition, while our results only include the gas-phase influences of PSCs in August, there is still a possibility that PSC sedimentation influences surface level TNIT in early austral spring by particulate deposition.

Sensitivity calculations show that the modeled background concentrations are mostly affected by TNIT produced in the free troposphere over mid latitudes ($30°S–65°S$) through the reaction $NO_2 + OH \rightarrow HNO_3$. NO_x for the reaction is mainly supplied from fossil fuel combustion, soil, lightning, and thermal decomposition and photolysis of PAN. It is evident from horizontal sensitivity maps that surface level Antarctica receives more influences from outside Antarctica during winter than summer. August is a transitional month; thus, the modeled August peak is comparably affected by tropospheric and stratospheric sources. In summer, surface level TNIT is negatively sensitive to stratospheric gas-phase chemistry that consumes NO_x, HNO_3, and HNO_4 in the stratosphere. Thus TNIT concentrations decrease in summer even though total emissions from south of $15°S$ increase. Given that the model lacks post-depositional processing, photochemical decomposition of PAN accounts for the largest fraction of NO_x supply for the HNO_3 forming reaction during the austral summer.

Acknowledgments

References

Alexander, B., Hastings, M.G., Allman, D.J., Dachs, J., Thornton, J.A., Kunasek, S.A., 2009. Quantifying atmospheric nitrate formation pathways based on a global model of the oxygen isotopic composition ($\delta^{17}O$) of atmospheric nitrate. Atmospheric Chemistry and Physics 9, 5043–5056.

Arthern, R.J., Winebrenner, D.P., Vaughan, D.G., 2006. Antarctic snow accumulation mapped using polarization of 4.3-cm wavelength microwave emission. Journal of Geophysical Research: Atmospheres 111.

Bey, I., Jacob, D.J., Yantosca, R.M., Logan, J.A., Field, B.D., Fiore, A.M., Li, Q., Liu, H.Y., Mickley, L.J., Schultz, M.G., 2001. Global modeling of tropospheric chemistry with assimilated meteorology: Model description and evaluation. Journal of Geophysical Research: Atmospheres 106, 23,073–23,095.

Binkowski, F.S., Roselle, S.J., 2003. Models-3 community multiscale air quality (CMAQ) model aerosol component 1. Model description. Journal of Geophysical Research: Atmospheres 108, 4183.

Capps, S.L., Henze, D.K., Hakami, A., Russell, A.G., Nenes, A., 2012. ANISORROPIA: the adjoint of the aerosol thermodynamic model ISORROPIA. Atmospheric Chemistry and Physics 12, 527–543.

Carslaw, K.S., Luo, B., Peter, T., 1995. An analytic expression for the composition of aqueous HNO_3-H_2SO_4 stratospheric aerosols including gas phase removal of HNO_3. Geophysical Research Letters 22, 1877–1880.

Carslaw, K.S., Luo, B.P., Clegg, S.L., Peter, T., Brimblecombe, P., Crutzen, P.J., 1994. Stratospheric aerosol growth and HNO_3 gas phase depletion from coupled HNO_3 and water uptake by liquid particles. Geophysical Research Letters 21, 2479–2482.

Chin, M., Ginoux, P., Kinne, S., Torres, O., Holben, B.N., Duncan, B.N., Martin, R.V., Logan, J.A., Higurashi, A., Nakajima, T., 2002. Tropospheric aerosol optical thickness from the GOCART model and comparisons with satellite and sun photometer measurements. Journal of the Atmospheric Sciences 59, 461–483.

Fahey, D.W., Kelly, K.K., Kawa, S.R., Tuck, A.F., Loewenstein, M., Chan, K.R., Heidt, L.E., 1990. Observations of denitrification and dehydration in the winter polar stratospheres. Nature 344, 321–324.

Fairlie, T.D., Jacob, D.J., Park, R.J., 2007. The impact of transpacific transport of mineral dust in the united states. Atmospheric Environment 41, 1251–1266.

Henze, D.K., Hakami, A., Seinfeld, J.H., 2007. Development of the adjoint of geos-chem. Atmospheric Chemistry and Physics 7, 2413–2433.

Henze, D.K., Seinfeld, J.H., Shindell, D.T., 2009. Inverse modeling and mapping us air quality influences of inorganic $PM_{2.5}$ precursor emissions using the adjoint of GEOS-Chem. Atmospheric Chemistry and Physics 9, 5877–5903.

Jacobi, H.W., Weller, R., Jones, A., Anderson, P., Schrems, O., 2000. Peroxyacetyl nitrate (PAN) concentrations in the Antarctic troposphere measured during the photochemical experiment at Neumayer (PEAN'99). Atmospheric Environment 34, 5235–5247.

Jiang, Z., Jones, D.B.A., Kopacz, M., Liu, J., Henze, D.K., Heald, C., 2011. Quantifying the impact of model errors on top-down estimates of carbon monoxide emissions using satellite observations. Journal of Geophysical Research: Atmospheres 116, D15306.

Jones, A.E., Wolff, E.W., Ames, D., Bauguitte, S.J., Clemitshaw, K.C., Fleming, Z., Mills, G.P., Saiz-Lopez, A., Salmon, R.A., Sturges, W.T., Worton, D.R., 2011. The multi-seasonal NOy budget in coastal Antarctica and its link with surface snow and ice core nitrate: results from the CHABLIS campaign. Atmospheric Chemistry and Physics 11, 9271–9285.

Jones, A.E., Wolff, E.W., Salmon, R.A., Bauguitte, S.J., Roscoe, H.K., Anderson, P.S., Ames, D., Clemitshaw, K.C., Fleming, Z.L., Bloss, W.J., Heard, D.E., Lee, J.D., Read, K.A., Hamer, P., Shallcross, D.E., Jackson, A.V., Walker, S.L., Lewis, A.C., Mills, G.P., Plane, J.M.C., Saiz-Lopez, A., Sturges, W.T., Worton, D.R., 2008. Chemistry of the Antarctic boundary layer and the interface with snow: an overview of the CHABLIS campaign. Atmospheric Chemistry and Physics 8, 3789–3803.

Jourdain, B., Legrand, M., 2002. Year-round records of bulk and size-segregated aerosol composition and HCl and HNO_3 levels in the dumont d'Urville (coastal Antarctica) atmosphere: implications for sea-salt aerosol fractionation in the winter and summer. Journal of Geophysical Research: Atmospheres 107. ACH 20-13–ACH 20-21.

Kopacz, M., Jacob, D.J., Fisher, J.A., Logan, J.A., Zhang, L., Megretskaia, I.A., Yantosca, R.M., Singh, K., Henze, D.K., Burrows, J.P., Buchwitz, I., McMillan, W.W., Gille, J.C., Edwards, D.P., Eldering, A., Thouret, V., Nedelec, P., 2010. Global estimates of CO sources with high resolution by adjoint inversion of multiple satellite datasets (MOPITT, AIRS, SCIAMACHY, TES). Atmospheric Chemistry and Physics 10, 855–876.

Kopacz, M., Mauzerall, D.L., Wang, J., Leibensperger, E.M., Henze, D.K., Singh, K., 2011. Origin and radiative forcing of black carbon transported to the Himalayas and Tibetan plateau. Atmospheric Chemistry and Physics 11, 2837–2852.

Krinner, G., Genthon, C., 2003. Tropospheric transport of continental tracers towards Antarctica under varying climatic conditions. Tellus B 55, 54–70.

Legrand, M., Lorius, C., Barkov, N., Petrov, V., 1988. Vostok (Antarctica) ice core: Atmospheric chemistry changes over the last climatic cycle (160,000 years). Atmospheric Environment 22, 317–331.

Legrand, M.R., Kirchner, S., 1990. Origins and variations of nitrate in south polar precipitation. Journal of Geophysical Research: Atmospheres 95, 3493–3507.

Liu, H., Jacob, D.J., Bey, I., Yantosca, R.M., 2001. Constraints from ^{210}Pb and ^7Be on wet deposition and transport in a global three-dimensional chemical tracer model driven by assimilated meteorological fields. Journal of Geophysical Research: Atmospheres 106, 12109–12128.

Liu, J.J., Jones, D.B.A., Worden, J.R., Noone, D., Parrington, M., Kar, J., 2009. Analysis of the summertime buildup of tropospheric ozone abundances over the middle east and north Africa as observed by the tropospheric emission spectrometer instrument. Journal of Geophysical Research: Atmospheres 114.

Mayewski, P.A., Legrand, M.R., 1990. Recent increase in nitrate concentration of Antarctic snow. Nature 346, 258–260.

Mayewski, P.A., Lyons, W.B., Spencer, M.J., Twickler, M., Dansgaard, W., Koci, B., Davidson, C.I., Honrath, R.E., 1986. Sulfate and nitrate concentrations from a south Greenland ice core. Science 232, 975–977. PMID: 17759282.

McLinden, C.A., Olsen, S.C., Hannegan, B., Wild, O., Prather, M.J., Sundet, J., 2000. Stratospheric ozone in 3-D models: A simple chemistry and the cross-tropopause flux. Journal of Geophysical Research: Atmospheres 105, 14653–14665.

Mills, G.P., Sturges, W.T., Salmon, R.A., Bauguitte, S.J., Read, K.A., Bandy, B.J., 2007. Seasonal variation of peroxyacetylnitrate (PAN) in coastal Antarctica measured with a new instrument for the detection of sub-part per trillion mixing ratios of PAN. Atmospheric Chemistry and Physics 7, 4589–4599.

Murray, L.T., Jacob, D.J., Logan, J.A., Hudman, R.C., Koshak, W.J., 2012. Optimized regional and interannual variability of lightning in a global chemical transport model constrained by LIS/OTD satellite data. Journal of Geophysical Research: Atmospheres 117.

Olivier, J.G.J., Van Aardenne, J.A., Dentener, F.J., Pagliari, V., Ganzeveld, L.N., Peters, J.A.H.W., 2005. Recent trends in global greenhouse gas emissions: Regional trends 1970–2000 and spatial distribution of key sources in 2000. Environmental Science 2, 81–99.

Park, R.J., Jacob, D.J., Chin, M., Martin, R.V., 2003. Sources of carbonaceous aerosols over the united states and implications for natural visibility. Journal of Geophysical Research: Atmospheres 108.

Park, R.J., Jacob, D.J., Field, B.D., Yantosca, R.M., Chin, M., 2004. Natural and trans-boundary pollution influences on sulfate-nitrate-ammonium aerosols in the United States: Implications for policy. Journal of Geophysical Research: Atmospheres 109.

Parrington, M., Palmer, P.I., Henze, D.K., Tarasick, D.W., Hyer, E.J., Owen, R.C., Helmig, D., Clerbaux, C., Bowman, K.W., Deeter, M.N., Barratt, E.M., Coheur, P.F.,

Hurtmans, D., Jiang, Z., George, M., Worden, J.R., 2012. The influence of boreal biomass burning emissions on the distribution of tropospheric ozone over north America and the north Atlantic during 2010. Atmospheric Chemistry and Physics 12, 2077–2098.

Paulot, F., Henze, D.K., Wennberg, P.O., 2012. Impact of the isoprene photochemical cascade on tropical ozone. Atmospheric Chemistry and Physics 12, 1307–1325.

Pitts, M.C., Thomason, L.W., Poole, L.R., Winker, D.M., 2007. Characterization of polar stratospheric clouds with spaceborne lidar: CALIPSO and the 2006 Antarctic season. Atmospheric Chemistry and Physics 7, 5207–5228.

Rankin, A.M., Wolff, E.W., 2003. A year-long record of size-segregated aerosol composition at Halley, Antarctica. Journal of Geophysical Research: Atmospheres 108.

Ritz, C., Rommelaere, V., Dumas, C., 2001. Modeling the evolution of Antarctic ice sheet over the last 420,000 years: Implications for altitude changes in the Vostok region. Journal of Geophysical Research: Atmospheres 106, 31943–31964.

Röthlisberger, R., Hutterli, M.A., Sommer, S., Wolff, E.W., Mulvaney, R., 2000. Factors controlling nitrate in ice cores: Evidence from the Dome C deep ice core. Journal of Geophysical Research: Atmospheres 105, 20,565–20,572.

Rubin, M.J., 1953. Seasonal variations of the Antarctic tropopause. Journal of Meteorology 10, 127–134.

Sauvage, B., Martin, R.V., van Donkelaar, A., Liu, X., Chance, K., Jaeglé, L., Palmer, P.I., Wu, S., Fu, T.M., 2007. Remote sensed and in situ constraints on processes affecting tropical tropospheric ozone. Atmospheric Chemistry and Physics 7, 815–838.

Savarino, J., Kaiser, J., Morin, S., Sigman, D.M., Thiemens, M.H., 2007. Nitrogen and oxygen isotopic constraints on the origin of atmospheric nitrate in coastal Antarctica. Atmospheric Chemistry and Physics 7, 1925–1945.

Savoie, D.L., Prospero, J.M., Larsen, R.J., Huang, F., Izaguirre, M.A., Huang, T., Snowdon, T.H., Custals, L., Sanderson, C.G., 1993. Nitrogen and sulfur species in Antarctic aerosols at Mawson, Palmer Station, and Marsh (King George Island). Journal of Atmospheric Chemistry 17, 95–122.

Stohl, A., Sodemann, H., 2010. Characteristics of atmospheric transport into the Antarctic troposphere. Journal of Geophysical Research: Atmospheres 115, 16.

Wagenbach, D., Legrand, M., Fischer, H., Pichlmayer, F., Wolff, E.W., 1998. Atmospheric near surface nitrate at coastal Antarctic sites. Journal of Geophysical Research: Atmospheres 103, 11007–11020.

Walker, T.W., Jones, D.B.A., Parrington, M., Henze, D.K., Murray, L.T., Bottenheim, J.W., Anlauf, K., Worden, J.R., Bowman, K.W., Shim, C., Singh, K., Kopacz, M., Tarasick, D.W., Davies, J., Gathen, P.v.d., Thompson, A.M., Carouge, C.C., 2012. Impacts of midlatitude precursor emissions and local photochemistry on ozone abundances in the Arctic. Journal of Geophysical Research: Atmospheres 117, D01305.

Wang, Y., Jacob, D.J., Logan, J.A., 1998. Global simulation of tropospheric O_3-NO_x – hydrocarbon chemistry 3. Origin of tropospheric ozone and effects of nonmethane hydrocarbons. Journal of Geophysical Research: Atmospheres 103, 10757–10,767.

Wecht, K.J., Jacob, D.J., Wofsy, S.C., Kort, E.A., Worden, J.R., Kulawik, S.S., Henze, D.K., Kopacz, M., Payne, V.H., 2012. Validation of TES methane with HIPPO aircraft observations: Implications for inverse modeling of methane sources. Atmospheric Chemistry and Physics 12, 1823–1832.

Weller, R., Jones, A.E., Wille, A., Jacobi, H.W., McIntyre, H.P., Sturges, W.T., Huke, M., Wagenbach, D., 2002. Seasonality of reactive nitrogen oxides (NO_y) at Neumayer station, Antarctica. Journal of Geophysical Research: Atmospheres 107, 4673.

Weller, R., Traufetter, F., Fischer, H., Oerter, H., Piel, C., Miller, H., 2004. Post-depositional losses of methane sulfonate, nitrate, and chloride at the European project for ice coring in antarctica deep-drilling site in Dronning Maud land, Antarctica. Journal of Geophysical Research: Atmospheres 109, D07301.

Weller, R., Wagenbach, D., Legrand, M., Elsässer, C., Tian-Kunze, X., König-Langlo, G., 2011. Continuous 25-yr aerosol records at coastal antarctica – i: Inter-annual variability of ionic compounds and links to climate indices. Tellus B 63, 901–919.

van der Werf, G.R., Morton, D.C., DeFries, R.S., Giglio, L., Randerson, J.T., Collatz, G.J., Kasibhatla, P.S., 2009. Estimates of fire emissions from an active deforestation region in the southern amazon based on satellite data and biogeochemical modelling. Biogeosciences 6, 235–249.

van der Werf, G.R., Peters, W., van Leeuwen, T.T., Giglio, L., 2013. What could have caused pre-industrial biomass burning emissions to exceed current rates? Climate of the Past 9, 289–306.

Wesely, M., 1989. Parameterization of surface resistances to gaseous dry deposition in regional-scale numerical models. Atmospheric Environment 23, 1293–1304.

Wilson, A.T., House, D.A., 1965. Fixation of nitrogen by aurora and its contribution to the nitrogen balance of the earth. Nature 205, 793–794.

Wolff, E.W., Bigler, M., Curran, M.a.J., Dibb, J.E., Frey, M.M., Legrand, M., McConnell, J.R., 2012. The Carrington event not observed in most ice core nitrate records. Geophysical Research Letters 39, L08503.

Wolff, E.W., Jones, A.E., Bauguitte, S.J.B., Salmon, R.A., 2008. The interpretation of spikes and trends in concentration of nitrate in polar ice cores, based on evidence from snow and atmospheric measurements. Atmospheric Chemistry and Physics 8, 5627–5634.

Yevich, R., Logan, J.A., 2003. An assessment of biofuel use and burning of agricultural waste in the developing world. Global Biogeochemical Cycle 17, 1095.

Zatko, M.C., Grenfell, T.C., Alexander, B., Doherty, S.J., Thomas, J.L., Yang, X., 2013. The influence of snow grain size and impurities on the vertical profiles of actinic flux and associated NOx emissions on the antarctic and greenland ice sheets. Atmospheric Chemistry and Physics 13, 3547–3567.

Zeller, E.J., Parker, B.C., 1981. Nitrate ion in Antarctic firn as a marker for solar activity. Geophysical Research Letters 8 (PP), 895–898.